International Conference on Lightning Protection
33rd International Conference on Lightning Protection
25 - 30 September 2016
Estoril, Portugal

Analysis on the Choosing of Test Electrode for Lightning Current Metal Ablation Experiments

Yakun Liu, Hailiang Xia, Zhengcai Fu
Department of Electrical Engineering
Shanghai Jiao Tong University
Shanghai, China
zcfu@sjtu.edu.cn

Xin Gao, Baoquan Liu
Qingdao Safety Engineering Institute
SINOPEC
Qingdao, China
Gaoxinhse@163.com

***Abstract*—Metal ablation area and depth are affected by electrodes used in simulated lightning metal ablation experiment. In this study, electrode materials are firstly investigated to decrease electrode jet. Then nine different shapes of experiment electrodes, which are hemisphere electrode, semi-ellipsoid electrode and cone electrode with three different diameters of 6, 8 and 10mm respectively, are used to investigate the influences on metal ablation results with simulated long continuing current. The results show that, using cone electrode leads to the severest metal ablation results both in ablation area and depth, followed by using semi-ellipsoid electrode and hemisphere electrode. For electrodes of same shape, metal ablation area and depth decrease with its diameter increasing. The different ablation results caused by different shapes of electrodes are properly explained with initial electric field strength distribution analysis, subsequent dynamic electron density and electron energy density distribution analysis by the finite-element numerical analysis software of ANASYS and COMSOL Multiphysics.**

Keywords- experiment electrode, simulated lightning current, metal ablation, electric field, electron energy.

I. INTRODUCTION

Direct effects of lightning on metallic materials are mainly melting or burning at attachment points. The metal ablation depth and area caused by lightning currents are important parameters for lightning protection of aircrafts, large floating oil tanks and so on. Due to the complex processes involved in metal ablation, experiment method is an effective way and lots of researches based on metal ablation experiment have been conducted [1-7]. However, electrodes of different shapes are used in those researches, such as rod electrode with hemisphere head, "L" shaped electrode, "Pressing" electrode etc., which makes it inaccurate to compare the existing results with different researches. Limited by the ability of simulated lightning generator, short air gap discharge is usually adopted to generate the arc to simulate lightning channel in metal ablation experiment, in which electrodes have a significant influence on ablation area and depth. The influence has not been discussed and needs to be furtherly investigated.

In metal ablation experiment, it is fundamental to solve the problem of electrode jet properly [8-11]. Maecker [12] firstly gave the explanation of electrode jet based on magnetic self-compression in an arc and the development of a strong net longitudinal pressure gradient in the vicinity of arc root on electrode surface. W. Zischank [13] introduced Maecker's theory into lightning technology and established a standard test configuration, of which a heat resistant dielectric restrictor aperture on electrode and a fine copper guide wire of 0.1mm diameter terminated 10mm above the sample are used. A. Kern [14] investigated the influence of insulating counter electrode with a Teflon at its top, aiming to decrease plasma jet, on metal ablation by comparing it with standard electrode. The research results showed that ablation volume caused by using insulating electrode were only 40% to 60% of that by using standard electrode. In conclusion, using insulating electrode solves the electrode jet problem, but it decreases electric field strength and limits the arc energy, which reduces ablation volume.

In this paper, to decrease electrode jet, firstly, based on material's anti-erosion capabilities analysis, a kind of electrode materials W80 (mass fraction 80% tungsten and 20% copper) is manufactured and the manufacturing process of copper permeated in sintered tungsten skeleton under high temperature atmosphere is adopted to improve material's compactness. This direct electrode successfully reduces electrode jet without ablation volume decreasing. Then nine different shapes of electrodes, which are hemisphere electrode, semi-ellipsoid electrode and cone electrode with three different diameters of 6, 8 and 10mm respectively, are used to investigate the impacts of electrode shapes on metal ablation depth and area with simulated long continuing current experiment. In the end, the finite-element numerical analysis (FEA) software of ANASYS and COMSOL Multiphysics are adopted to analyze initial electric field strength distribution, subsequent dynamic electron density and energy density distribution to explain the difference of metal ablation depth and area caused by different shapes of electrodes in the experiment.

Project Supported by Natural Science Foundation of China (51577117).

II. EXPERIMENTAL METHODS

A. Experiment electrode

Electrode jet phenomenon is the interaction of jets of ions and vaporized material originating from the electrode surface caused by electrode melting. So increasing electrode material's anti-erosion capability is a good way to reduce the influence of electrode jet. Material's anti-erosion capability is determined by its physical properties, such as melting point, density, specific heat capacity, thermal conductivity and so on, which can be calculated by Equation (1) [17].

$$R=T(\rho c\lambda)^{1/2} \quad (1)$$

Where T is melting point (℃), ρ is density ($g\cdot cm^{-3}$), c is specific heat capacity ($J\cdot g^{-1}\cdot ℃^{-1}$), λ is thermal conductivity ($W\cdot cm^{-1}\cdot ℃^{-1}$).

The calculation results of several common materials' anti-erosion capability are shown in Table I.

TABLE I. ANTI-EROSION CAPABILITY OF COMMON MATERIALS

Material	T ℃	ρ $g\cdot cm^{-3}$	C $J\cdot g^{-1}\cdot ℃^{-1}$	λ $W\cdot cm^{-1}\cdot ℃^{-1}$	*R*
aluminum(Al)	658	2.70	0.904	2.03	1567
Copper(Cu)	1083	8.93	0.384	4.00	4011
Iron(Fe)	1527	7.80	0.447	0.82	2581
Tungsten(W)	3415	19.25	0.138	1.70	7257

From the results, it can be concluded that tungsten material has the highest anti-erosion capability compared with copper, iron and aluminum. However, tungsten material has a low electric conductivity and thermal conductivity, which lead to a high temperature rise in partial area on electrode. And it is hard to process. So tungsten material is not suitable for experiment electrode. Combined the tungsten material's advantages of high melting point and anti-erosion capability with the copper material's advantages of good electric and thermal conductivity, tungsten copper alloy performs a good characteristics of high melting point, good anti-erosion capability, fine electric and thermal conductivity, which is suitable for metal ablation experiment. Besides it is easier to process. So the tungsten copper alloy is chosen as the experiment electrode material.

The tungsten-copper binary phase diagram shows that tungsten copper alloy of tungsten mass fraction in excess of 70% approximately reaches the saturated gasification point. To increase the alloy material's electric conductivity and thermal conductivity, it is a good method to increase copper mass fraction in tungsten copper alloy. In the experiment, W80 consisted of mass fraction 80% tungsten and 20% copper is chosen as the electrode material, which has as considerable anti-erosion capability (R=7091) as tungsten (R=7257) and better performance on high melting point(2986℃), big density ($15.19g\cdot cm^{-1}$) and good thermal conductivity($2.35W\cdot cm^{-1}\cdot ℃^{-1}$). The alloy material's performance is partly determined by its compactness. To enhance W80 material's compactness, manufacturing process of copper permeated in sintered tungsten skeleton under high temperature atmosphere is adopted.

To investigate the impacts of electrode shapes on metal ablation depth and area, nine different shapes of electrodes, which are hemisphere electrode, semi-ellipsoid electrode and cone electrode with three different diameters of 6, 8 and 10mm respectively, are designed. Three different shapes of electrodes are shown in Figure 1 and different electrode curvature radius are measured in Table II.

Figure 1. Three kinds of electrodes

TABLE II. THE ELECTRODE CURVATURE RADIUS

electrode shape	**curvature radius/mm**	**electrode shape**	**curvature radius/mm**
10 mm hemisphere	5.0	6 mm semi-ellipsoid	1.2
8 mm hemisphere	4.0	10 mm cone	0.8
6 mm hemisphere	3.0	8 mm cone	0.5
10 mm semi-ellipsoid	2.0	6 mm cone	0.1
8 mm semi-ellipsoid	1.6		

B. Simulated lightning current

The most common simulated lightning current waveforms for metal ablation experiment are the ABCD waveforms defined in aircraft lightning experiment standard [9]. The current component A, B, C, and D are used to simulate the first return stroke current, continuing current of interval stoke, long continuing current and subsequent return stroke current, respectively. A-component in lightning has a peak amplitude of 200kA(±10%) and an action integral of $2\times10^6A^2\cdot s$ (±20%) with a total time duration not exceeding 500 microseconds. B-component in lightning has an average amplitude of 2kA(± 10%) flowing for a maximum duration of 5 milliseconds and a maximum charge transfer of 10C. C-component in lightning is a continuous component associated with the propagation of the lightning discharge in atmosphere. The standardized waveform requires the charge transfer of 200C with current intensities ranging between 200A and 800A. D-component in lightning has a peak amplitude of 100kA (±10%) and an action integral of $0.25\times10^6A^2\cdot s$ (±20%).

Based on the previous work [17], electrode shape has an obvious influence on metal ablation results for C-component in lightning. There is little influence of test electrode shapes for A, B and D components in lightning. So in this paper, the experiment is only carried out with simulated C-component, which has an amplitude of 384A, lasting 520ms. The simulated C-component in lightning is shown in Figure 2 (Sensing resistance is 1Ω in current measurement).

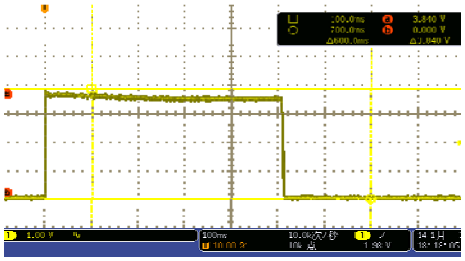

Figure 2. Simulated C-component in lightning

C. *Sample metal and experimental platform*

Aluminum material has a lower melting point (658℃), lower Mohs hardness (2.75) and better thermal conductivity (2.03 $W \cdot cm^{-1} \cdot ℃^{-1}$) than copper, iron and other metal materials, which is more sensitive in ablation depth and area. So Al 3003 is adopted in this research. Considering the previous ablation results and ultrasonic detection requirement, Al 3003 samples are processed into square of 150×150mm in plane, and 4mm in thickness, as shown in Figure 3.

Figure 3. Photograph of the test sample

The lightning ablation results are affected by arc root mobility and its structure on material surface, which strongly depend on electrode gap. W. Zischank [13], F.Uhlig [15] and A.M. Gouega [18] studied the influence of electrode gap and concluded that ablation volume decreased with electrode gap larger. It is also found that for cathodic configuration, the arc root had a continuous motion when experimental gap exceeded 10mm [15]. In order to get an accurate comparison of ablation results with electrodes of different shapes, the electrode gap is fixed at 10mm, under which the arc root does not move.

To prevent sample deformation caused by electrodynamics force, clamping device is designed and made of Bakelite resin material, as shown in Figure 4. The arc root on Al sample tends to be too mobile to melt the strands because of electromagnetic force induced by the current flowing through it. Accordingly, down conductors are connected to both sides of experimental platform to divert the arc current to ground symmetrically so that arc root cannot move easily.

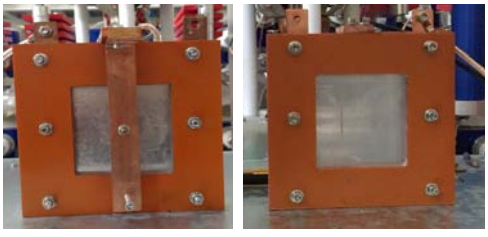

a. Front-face b. Back-face

Figure 4. The clamping device

Experimental condition is recorded in Table III. To improve experiment accuracy, every piece of Al 3003 sample is cleaned before experiment and used only once. In order to reduce the influence of discharge dispersion, every experiment is carried out for three times and the average results of three trials are recorded. The experiment time interval is controlled to cool down electrode to normal temperature. Electrode is processed again to erase metal oxide on surface after every experiment.

TABLE III. THE EXPERIMENTAL CONDITION

Temperature	Relative humidity	Atmospheric pressure	Elevation
12~15℃	15%	1.01×10^5Pa	4m

III. EXPERIMENT RESULTS AND ANALYSIS

A. *Experiment results*

In metal ablation experiment, metal ablation depth and area are measured by ultrasonic detection. The experiment results are shown in Table IV and Figure 5. Due to the thickness of aluminum plate is 4mm, if it is burnt through, the ablation depth is recorded as 4mm. The typical results can be seen in Figure 6, in which the electrodes with same diameter 8mm are adopted.

TABLE IV. COMPARED WITH METAL ABLATION AREA AND DEPTH OF DIFFERENT ELECTRODES

electrode shape	curvature radius/mm	ablation area/mm^2	ablation depth/mm
10 mm hemisphere	5.0	128.68	1.8
8 mm hemisphere	4.0	133.10	2.3
6 mm hemisphere	3.0	176.71	3.0
10 mm semi-ellipsoid	2.0	153.94	2.2
8 mm semi-ellipsoid	1.6	201.06	3.1
6 mm semi-ellipsoid	1.2	226.98	3.6
10 mm cone	0.8	265.90	3.4
8 mm cone	0.5	306.85	4.0 (burnt through)
6 mm cone	0.1	295.59	4.0 (burnt through)

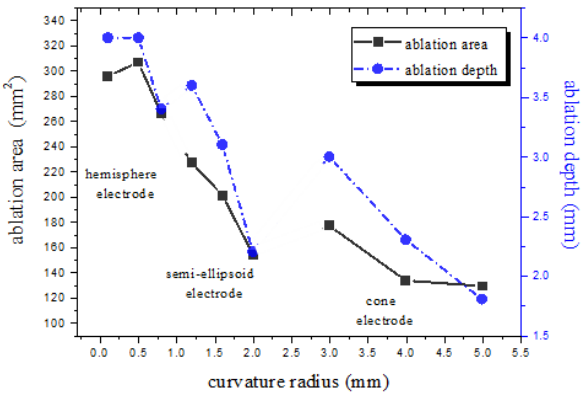

Figure 5. Compared with ablation area and depth of different electrodes

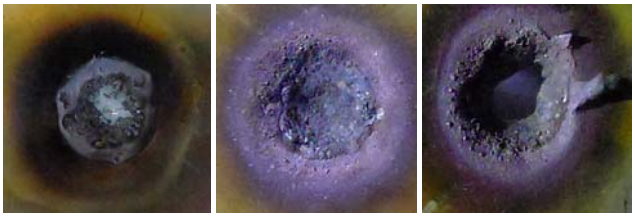

a. Hemisphere electrode b. Semi-ellipsoid electrode c. Cone electrode

Figure 6. Compared with metal ablation results of different electrodes

From experiment results, it can be concluded that for C-component in lightning, electrode shape has a big influence on metal ablation depth and area. Using cone electrode leads to the severest metal ablation results both in area and depth, followed by using semi-ellipsoid electrode and hemisphere electrode. Al 3003 sample is burnt through when cone electrode of diameter 8mm is used in experiment, which is at least 42.5% deeper than that of 2.3mm caused by using hemisphere electrode with the same diameter. And the ablation depth is 3.1mm with using semi-ellipsoid electrode of the same diameter. For ablation area, using cone electrode of diameter 8mm leads to ablation area of 306.85mm^2, which is higher than the ablation area 201.06 and 133.10mm^2 caused by using semi-ellipsoid electrode and hemisphere electrode of the same diameter, respectively.

For electrodes of the same shape, both metal ablation depth and area decrease with electrode curvature radius larger. For electrode shape of semi-ellipsoid, using electrode of curvature radius 1.2mm leads to ablation area 226.98mm^2, while the results are 201.06 and 153.94mm^2 corresponding to using electrode of curvature radius 1.6 and 2.0mm, respectively. And for ablation depth caused by using semi-ellipsoid electrode, the results are 3.6, 3.1 and 2.2mm corresponding to using electrode of curvature radius 1.2, 1.6 and 2.0mm, respectively.

B. Theory Analysis

From the experiment results, for C-component in lightning, electrode shapes have a significant influence on metal ablation depth and area. Ablation energy is mainly consisted of electric arc energy and Joule heat. The Joule heat Q_I is expressed by Equation (2).

$$Q_I = R\int i^2 dt \qquad (2)$$

The electric arc energy W can be deduced by Equation (3).

$$W = \int uidt = uQ = Q\int Eds \qquad (3)$$

Where, Q is the quantity of electric charge flowing through Al 3003 sample. E is electric field strength corresponding to ds. s is electrode gap.

As there is no difference in current amplitude and quantity of transferred charge, Joule heat is the same among different shapes of electrodes. Different ablation depth and area results are caused by different electric arc energy. From Equation (3), the electric arc energy is determined by electric field strength with the same charge transfer. Electrodes with different shapes have different electric field strength distribution. So FEA software of ANASYS is adopted to analyze the electric field strength distribution on electrode surface based on the ture-type model. The gap distance between electrode and Al 3003 sample surface is 10mm. The calculation model is shown in Figure 7 (taking cone electrode of diameter 10mm as an example). By applying unit voltage on different electrodes, the calculation results are show in Figure 8 (electrodes of 8mm diameter).

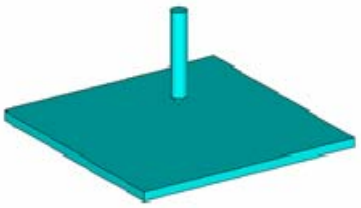

Figure 7. Calculation model

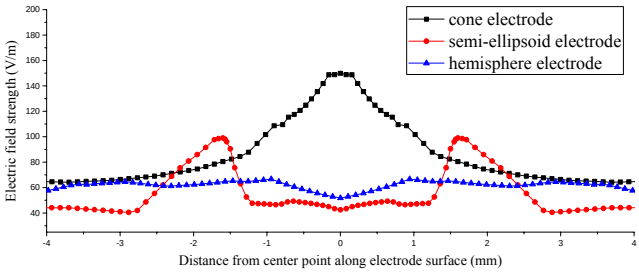

Figure 8. Electric field distribution of different electrodes (8mm diameter)

From calculation results, it can be concluded that, on initial stage, the electric field strength along electrode surface of cone electrode is much higher than that of semi-ellipsoid electrode and hemisphere electrode. So using cone electrode generates the strongest initial electric arc energy, which is almost 3 times higher than that of semi-ellipsoid electrode.

On subsequent arc development stage, electric field strength distribution is dynamic with arc moving forward due to electronic's dynamic redistribution. Hence in this paper, FEA software of COMSOL Multiphysics is used to investigate the electron density and electron energy density during arc development stage. A two-dimensional coupled model combined plasma dynamics and neutral gas flow is employed. Steady state equations are solved for neutral gas flow, and then the obtained stationary flow field results are coupled to the time-dependent solver for plasma dynamic. Three modules of electron drifting, heavy particles and stationary electric field analysis are employed in simulation. A pulsed negative polarity DC voltage of 7.5kV is applied on electrode. The gap distance between electrode and Al 3003 sample surface is 10mm. The air mixing ratio is 79% N_2 and 21% O_2 in the electrode gap. The initial electron density in the air is $10^6$1/m^3. Stremer discharge happens when electron density electron avalanches are of the order of $10^8$1/m^3, plasma can develop streamers to bridge the gap between cathode and anode [19]. Electron density and electron energy density are calculated. The derivation results at a certain time are shown in Figure 9 to Figure 14 (taking electrodes of diameter 6mm as an example).

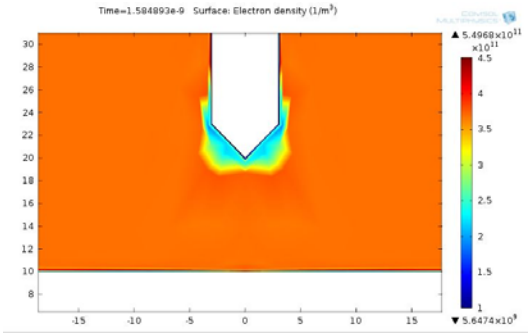

Figure 9. Electron density distribution of cone electrode

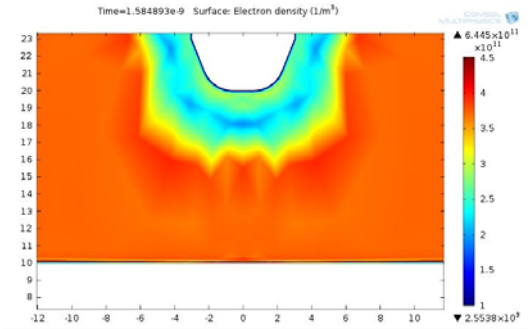

Figure 10. Electron density distribution of semi-ellipsoid electrode

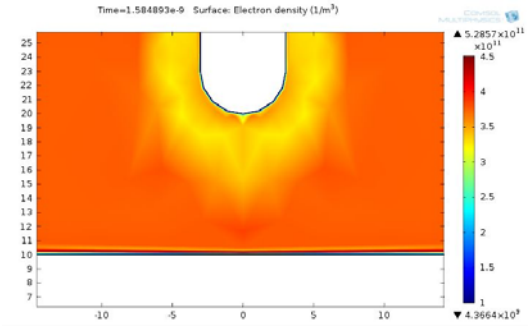

Figure 11. Electron density distribution of hemisphere electrode

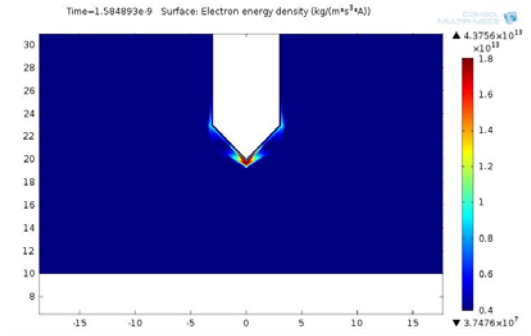

Figure 12. Electron energy density distribution of cone electrode

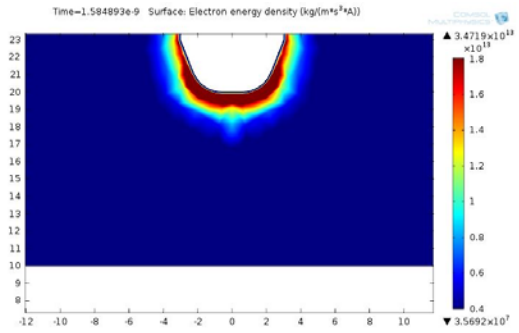

Figure 13. Electron energy density distribution of semi-ellipsoid electrode

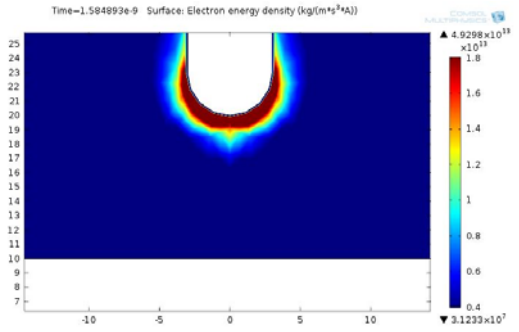

Figure 14. Electron energy density distribution of hemisphere electrode

From the derivation results, it can be concluded that, on arc development stage, using cone electrode generates a more concentrated electron density and electron energy density distribution, which leads to a more concentrated electric arc energy transmitting to metal sample. And the electron density and electron energy density are much higher with using cone electrode than that with using semi-ellipsoid electrode and hemisphere electrode.

Due to the strongest initial electric are energy and most highest electron energy density, using cone electrode leads to the severest ablation depth and area, followed by using semi-ellipsoid electrode and hemisphere electrode, which gains the coincident conclusions with the above experiment.

IV. CONLUSIONS

In this paper, both experimental and numerical investigation on influence of test electrode on lightning metal ablation experiment are performed. It is concluded that,

(1) For C-component in lightning, using cone electrode causes the most serious metal ablation results both in area and depth, followed by using semi-ellipsoid electrode and hemisphere electrode. For electrodes of the same shape, both metal ablation depth and area decrease with electrode curvature radius larger.

(2) On initial stage, using cone electrode generates the highest electric field strength on electrode surface and the strongest initial electric arc energy, followed by using semi-ellipsoid electrode and hemisphere electrode. On arc

development stage, using cone electrode generates a more concentrated electron density and electron energy density distribution. The electron density and electron energy density are also much higher with using cone electrode than that with using semi-ellipsoid electrode and hemisphere electrode.

(3) Due to the strongest electric arc energy on initial stage and most highest electron energy density on arc development stage, using cone electrode leads to the severest ablation depth and area, followed by using semi-ellipsoid electrode and hemisphere electrode, which is coincident with experiment.

REFERENCES

[1] N. Kamihara, Y. Kamino. "Development of a High-Current Generator to Comply with Aircraft Lightning Environments and Related Test Waveforms," *Mitsubishi Heavy Industries Technical Review*, vol.48, pp. 51-53, Dec. 2011.

[2] I.A. Metwally, F. Heidler, and W. Zischank. "Measurement of the rear-face temperature of metals struck by lightning long duration currents" *European transactions on electrical power* vol.14, no.4, pp. 201-222, Jul, 2004.

[3] D. Morgan, C.J. Hardwick, S.J. Haigh, A.J. Meakins. "The Interaction of Lightning with Aircraft and the Challenges of Lightning Testing." *Lightning Hazards to Aircraft and Launchers, Journal Aerospace Lab*, vol.05, no.11, 2012.

[4] M.P. Paisios, C.G. Karagiannopoulos, P.D. Bourkas. "Estimation of the temperature rise in cylindrical conductors subjected to heavy 10/350μs lightning current impulses." *Electric Power Systems Research* vol.78, no.1, pp.80-87. Feb, 2007.

[5] L. Chemartin, P. Lalande, B. Peyrou, A. Chazottes. "Direct effects of lightning on aircraft structure: analysis of the thermal, electrical and mechanical constraints." *J. Aeros. Lab* 5, 2012.

[6] N. Kamihara, Y. Kamino, "Development of a High-Current Generator to Comply with Aircraft Lightning Environments and Related Test Waveforms," *Mitsubishi Heavy Industries Technical Review*, vol. 48, pp. 51-53, Dec. 2011.

[7] S. Takeo, H. Yoshiyasu, K. Hideaki, T. Nobuyuki, "Visualization of Lightning Impulse Current Discharge on CFRP Laminate," *Proc.* ICLP, 2014.

[8] Aircraft Lightning Environment and Related Test Waveforms Standard. EUROCAE ED-84, 1997-8.

[9] SAE International Aircraft Lightning Environment and Related Test Waveforms. ARP5412, 2005.

[10] M. A. Uman, "All About Lightning," Dover, pp. 88-89, 1986.

[11] V. Mazur. "Triggered Lightning Strikes to Aircraft and Natural Intracloud Discharges." *Journal of Geophysical Research*, vol.94, no.3, pp. 3311-3325, Mar, 1989.

[12] H. Maecker, "Plasmaströmungen in Lichtbögen infolge eigenmagnetischer Kompression." *Zeitschrift für Physik A Hadrons and Nuclei*, vol.141, no.1, pp.198-216, 1955.

[13] W.J. Zischank, F. Drumm, R.J. Fisher, et al. "Reliable simulation of metal surface penetration by lightning continuing currents," *International Aerospace and Ground Conference on Lightning and Static Electricity*, Sep.1995.

[14] A. Kern. "Simulation and measurement of melting effects on metal sheets caused by direct lightning strikes," *Proceedings of International Aerospace and Ground Conference on Lightning and Static Electricity*. 1991.

[15] F.Uhlig, P. Gondot, B. Lepetit, J.P. Chabrerie, P Testé, "Experimental simulations of lightning impacts on aeronautical structural materials," pp. 533-538

[16] C.M. Xie, S.H. Shang, X.H. Tan, T. Du, "Electrode erosion in high Pressure and high current discharges," *High Power Laser and Particle Beams*, vol.25, no.9, pp. 2182-2187, 2013.

[17] Y.K. Liu, Z.C. Fu, A.F. Jiang, Q.Z. Liu, B.Q. Liu, " Analysis and Experiment on the Influence Factor of Metal Ablation Caused by Multiple Lightning Impulse Currents," *Asia-Pacific International Conference on Lightning (APL), Nagoya, Japan*, 2015.

[18] A.M. Gouega, Ph. Teste, R. Andlauer, T. Leblanc, J.-P. Chabrerie, "Study of the electrode gap influence on electrode erosion under the action of an electric arc." *European Physical Journal Applied Physics* vol.11, no.2, pp. 111-122, 2000.

[19] J.J. Lowke, "Toward a new theory of electrical breakdown in air." *Proceedings of the XIX International Conference on Gas Discharges and Their Applications, Beijing, China,* Sep. 2012.